Science Advances
AAAS

Supplementary Materials for

Use of intercellular proximity labeling to quantify and decipher cell-cell interactions directed by diversified molecular pairs

Shuang Qiu *et al.*

Corresponding author: Peng Wu, pengwu@scripps.edu; Jie P. Li, jieli@nju.edu.cn

Sci. Adv. **8**, eadd2337 (2022)
DOI: 10.1126/sciadv.add2337

This PDF file includes:

Figs. S1 to S15
Table S1
Supplementary Methods

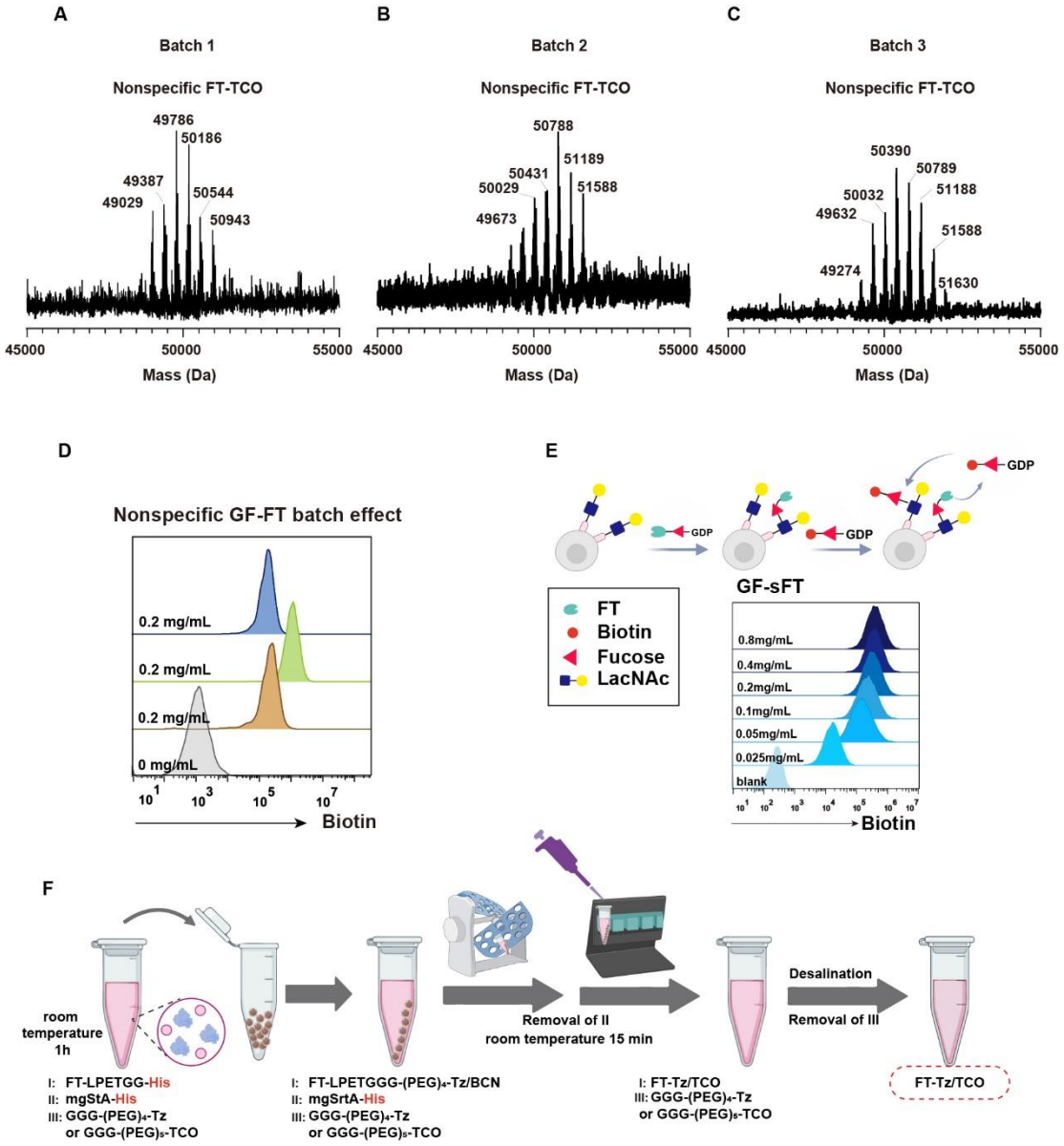

Fig. S1 The batch effects of GF-FT constructed by non-specific conjugation. Characterization of the batch effect of GF-FT by mass spectrum (A-C) and flow cytometry (D) (E) Self-Fucosyl-biotinylation of NK92 cells by cell-surface anchored FT. NK92 cells were first incubated under different concentrations of GF-sFT to install FT on cell surface, followed by wash and incubation with GF-Biotin. (F) The synthesis procedure of sFT.

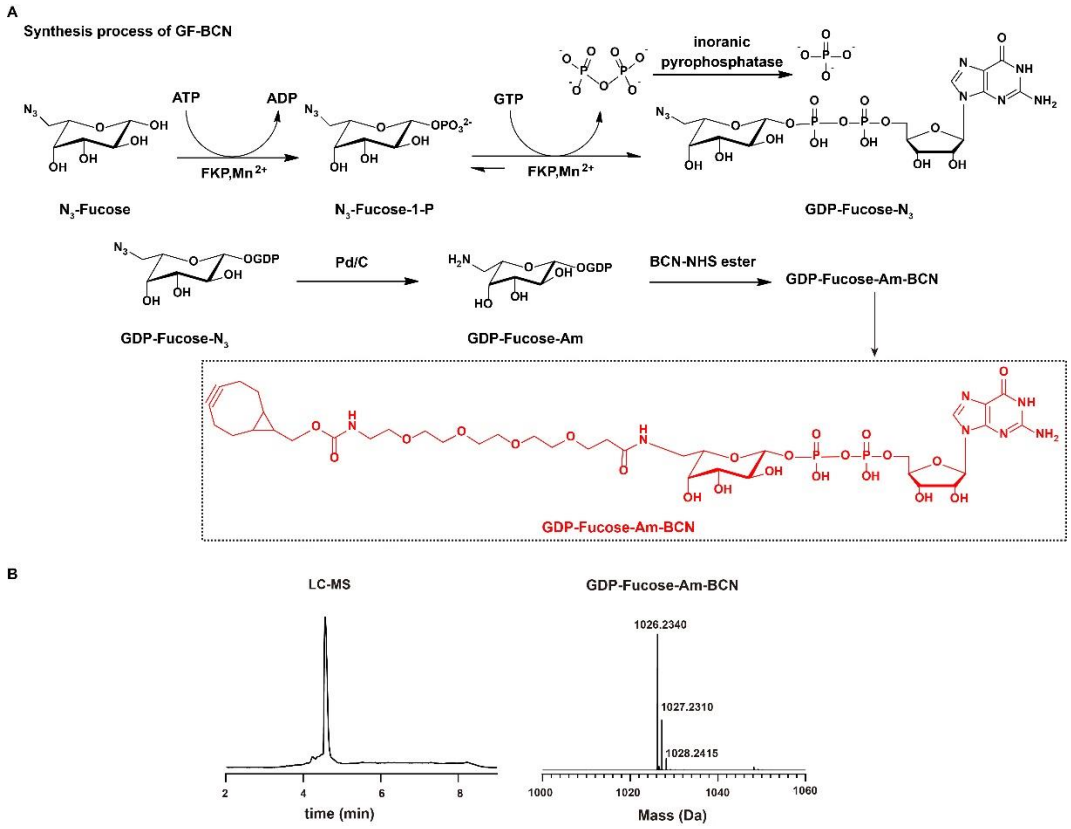

Fig. S2 Synthesis and characterization of GF-BCN.
(A) Synthesis procedure of GF-BCN. (B) Characterization of GF-BCN by mass spectrum.

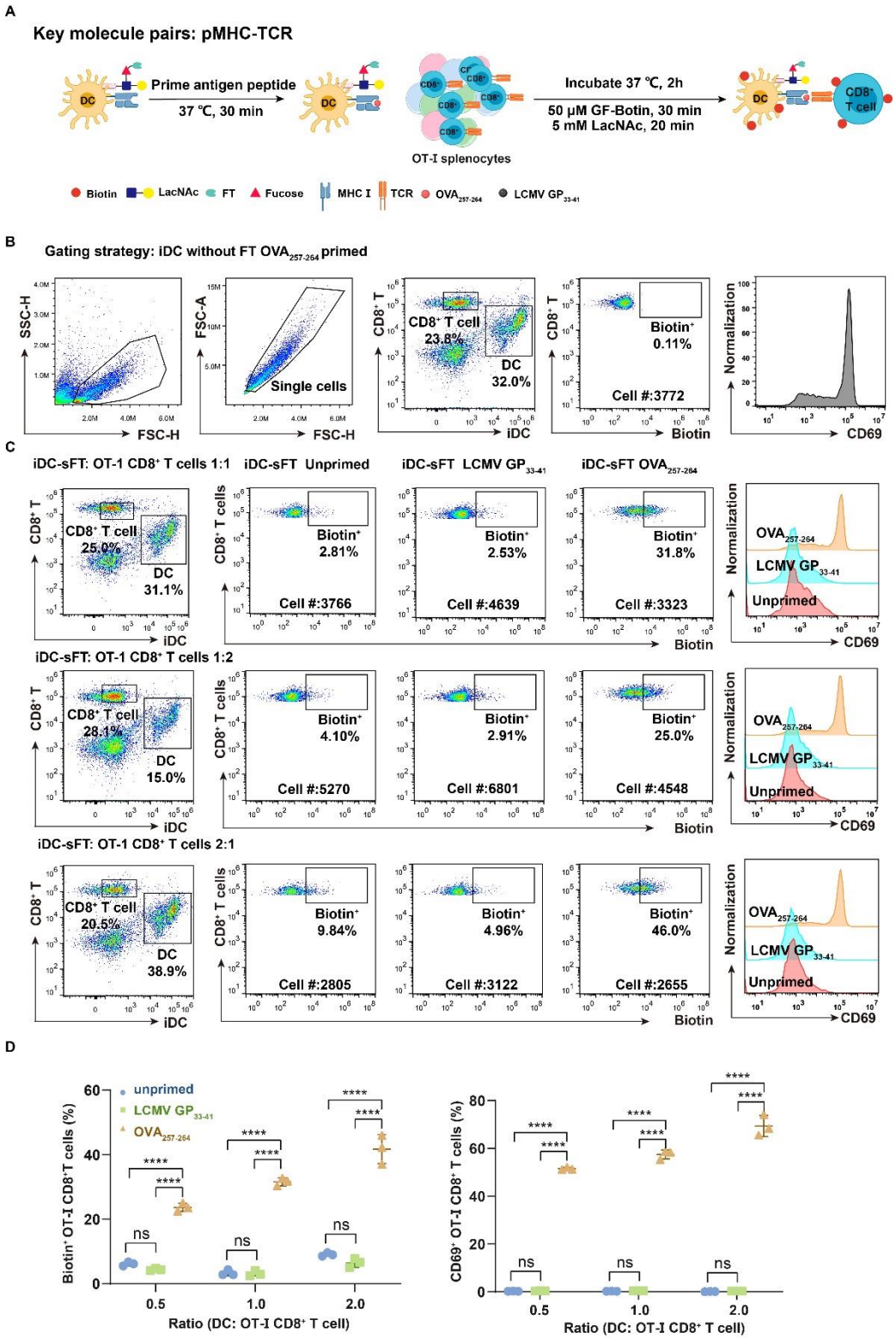

Fig. S3 Detection of MHC-antigen-TCR mediated interactions via iDC-sFT. (A) Workflow for probing MHC-antigen-TCR mediated interactions via iDC-sFT. (B) Gating strategy and representative flow cytometric plots showing the background of Fuc-Bio labeling (using iDC without FT as bait cell). (C) Flow cytometric plots and (D) statistics analysis showing antigen-specific biotinylation and CD69 activation of OT-I $CD8^+$ T cells under different ratios of bait cells versus prey cells. iDC: T cell ratio = 1: 1; 1: 2; 2: 1, n = 3. (ns $p > 0.05$; *$p < 0.05$; **$p < 0.05$; ****$p < 0.001$; ****$p < 0.0001$.)

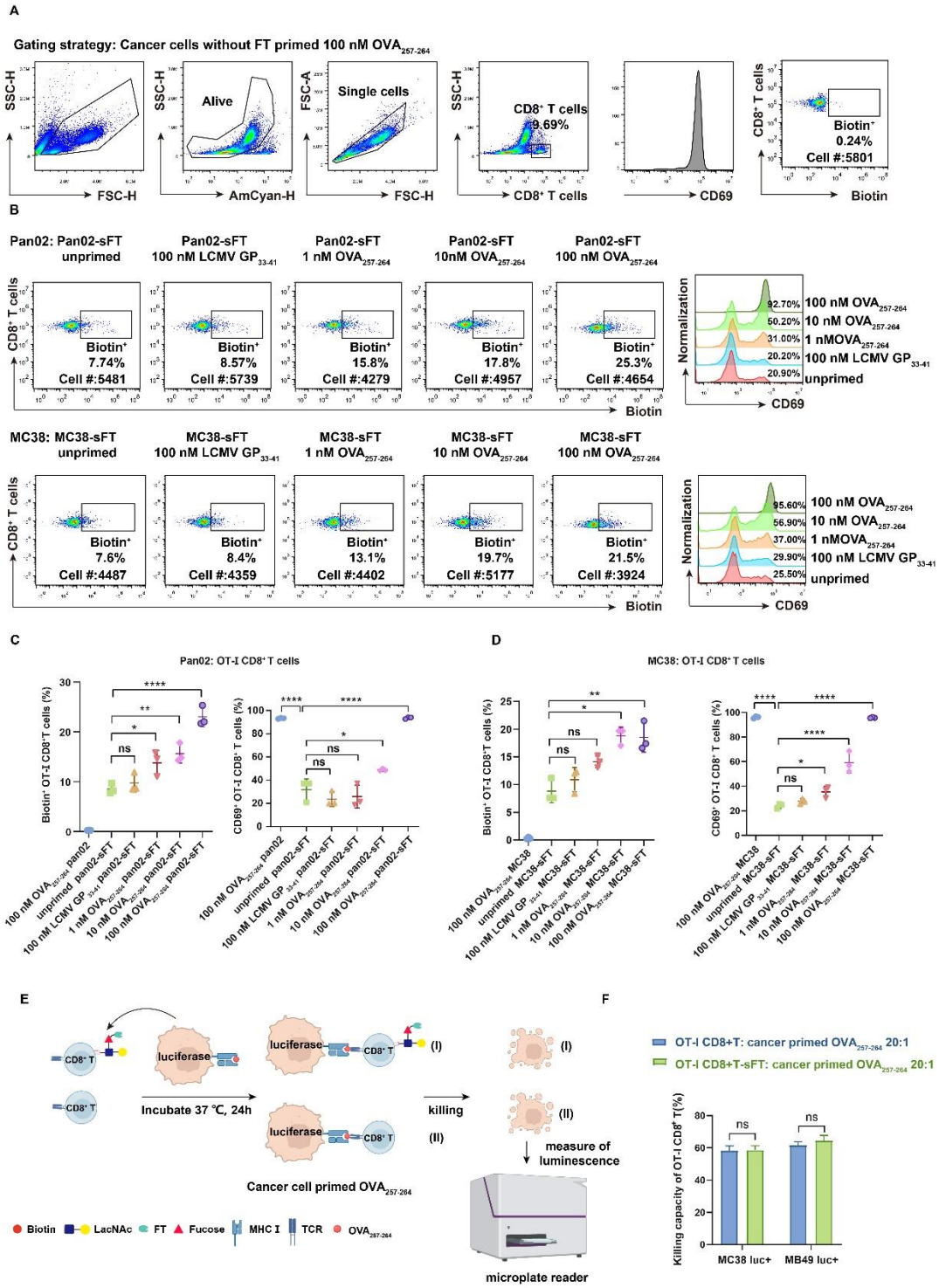

Fig. S4 Detection of MHC-antigen-TCR mediated interactions via cancer cell-sFT. (A) Gating strategy and representative flow cytometric plots showing background of Fuc-Bio labeling (using cancer cell without FT as bait cell). Flow cytometric plots (B) and statistics analysis (C-D) showing antigen-specific biotinylation and CD69 activation of OT-I $CD8^+$ T cells under different concentrations of $OVA_{257-264}$. (1 nM, 10 nM, 100 nM) Pan02 or MC38: T cell ratio = 1: 1, n = 3. (E) Schematic illustration of characterizing the killing ability of OT-I $CD8^+$ T cells against cancer cells pulsed with specific antigen. (F) Statistics showing of killing capacity of unlabeled and labeled OT-I $CD8^+$ T cells. (ns $p > 0.05$; *$p < 0.05$; **$p < 0.05$; ****$p < 0.001$; ****$p < 0.0001$.)

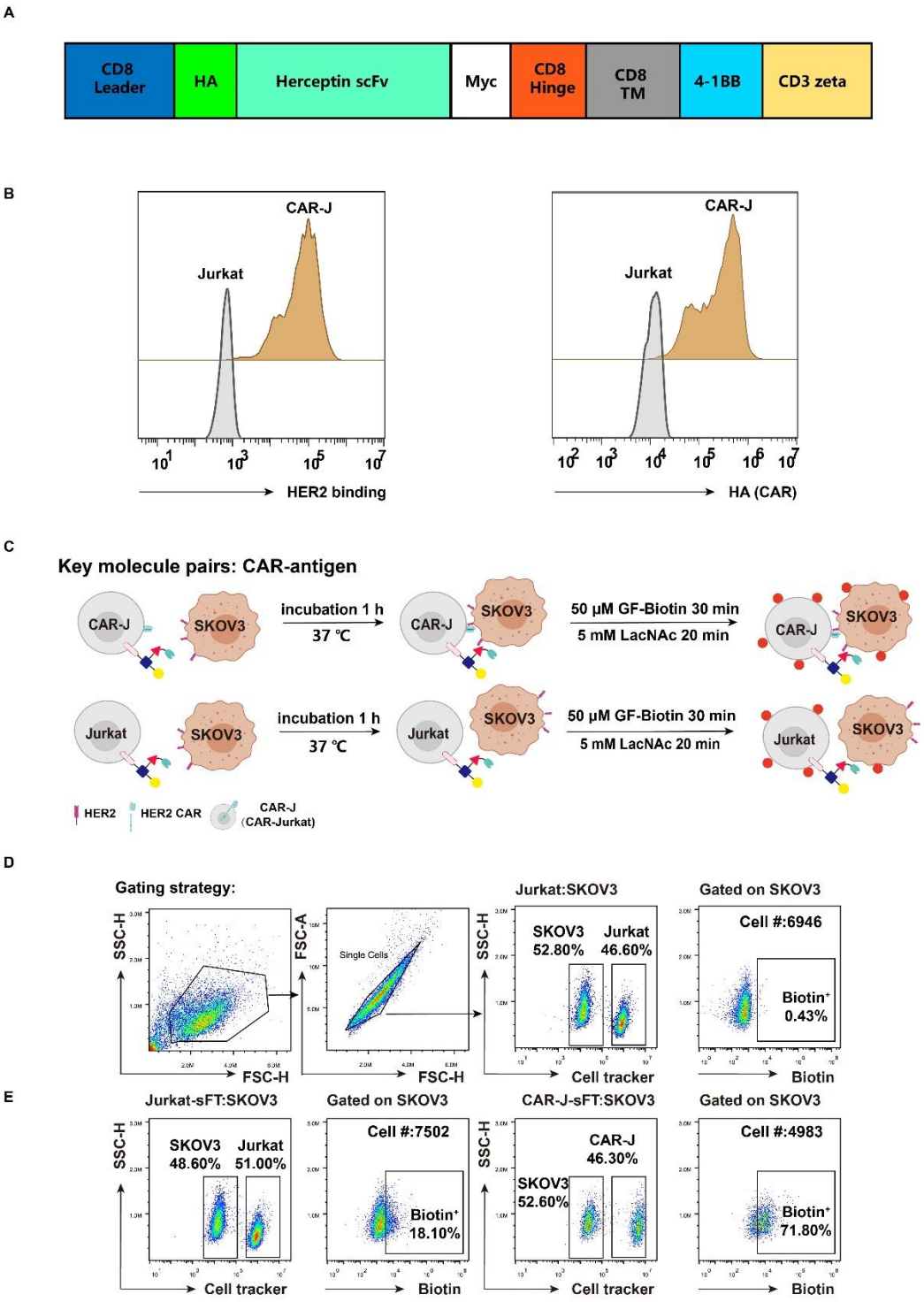

Fig. S5 Detection of CAR-antigen mediated interactions via Jurkat-sFT or CAR-J-sFT
(A) Schematic of CAR design. (B) Flow cytometric analysis of binding ability of CAR-J to HER2 and expression level of CAR on CAR-J. (C) Schematic workflow of detecting interactions between Jurkat/CAR-J and SKOV3 via Jurkat-sFT and CAR-J-sFT. (D) Gating strategy and representative flow cytometric plots showing the background of Fuc-Bio labeling (using Jurkat without FT as bait cell). (E) Representative flow cytometric plots showing biotinylation of SKOV3 using Jurkat-sFT and CAR-J-sFT. Jurkat/CAR-J: SKOV3 ratio = 1:1, n = 3. (ns $p > 0.05$; *$p < 0.05$; **$p < 0.05$; ****$p < 0.001$; ****$p < 0.0001$.)

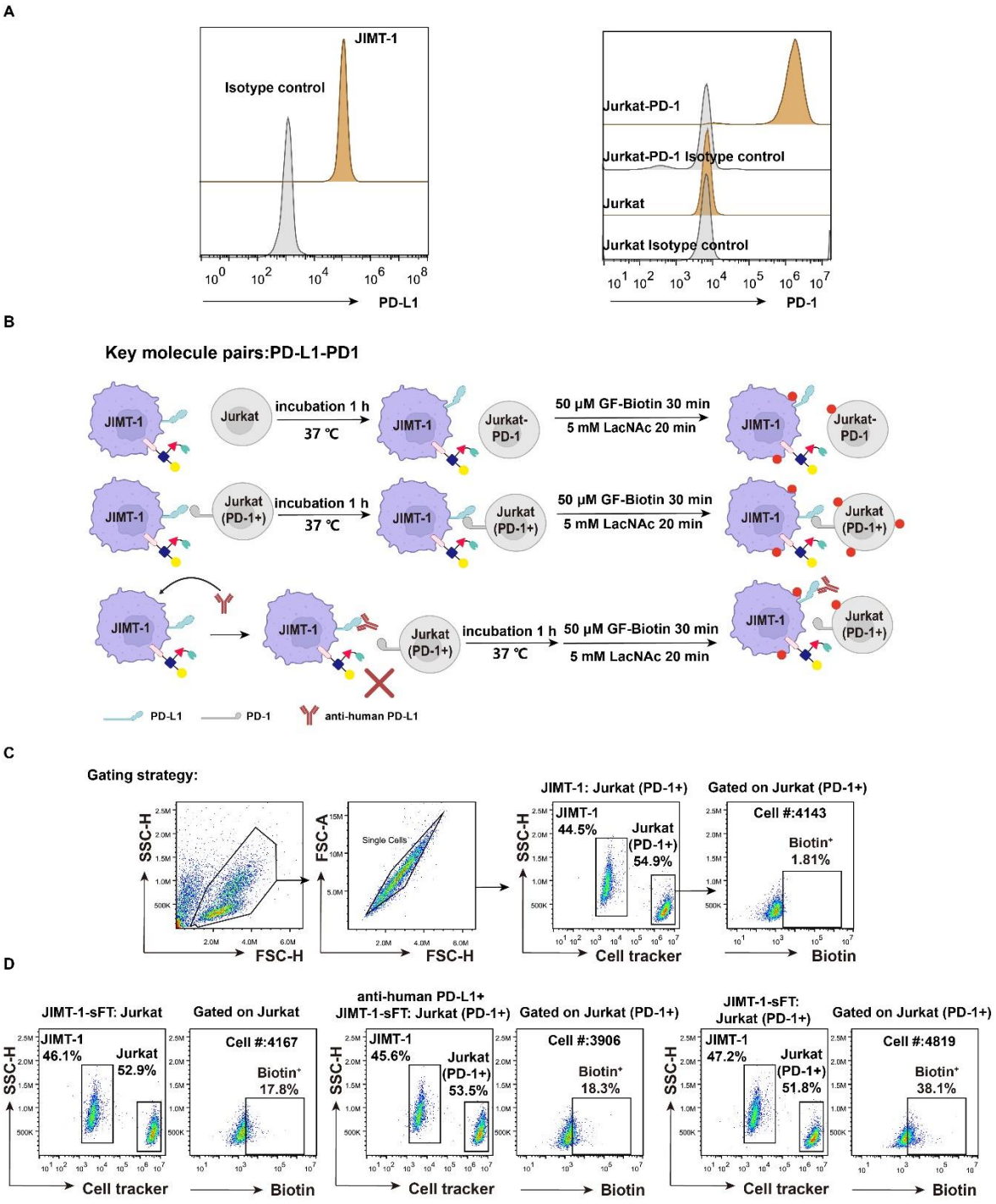

Fig. S6 Detection of PD-1-PD-L1 mediated interactions via JIMT-1-sFT. (A) Flow cytometric analysis of PD-L1 expression level on JIMT-1 and PD-1 expression level on Jurkat (PD-1+) and Jurkat. (B) Schematic workflow of detection interactions between Jurkat (PD-1+) /Jurkat and JIMT-1 via JIMT-1-sFT or JIMT-1-sFT pretreated by anti-human PD-L1. (C) Gating strategy and representative flow cytometric plots showing the background of Fuc-Bio labeling (using JIMT-1 without FT as bait cell). (D) Representative flow cytometric plots showing biotinylation of Jurkat (PD-1+) and Jurkat using JIMT-1-sFT or pretreated JIMT-1-sFT as bait cell. JIMT-1: Jurkat (PD-1+) ratio=1:1, n=3. (ns $p > 0.05$; *$p < 0.05$; **$p < 0.05$; ****$p < 0.001$; ****$p < 0.0001$.)

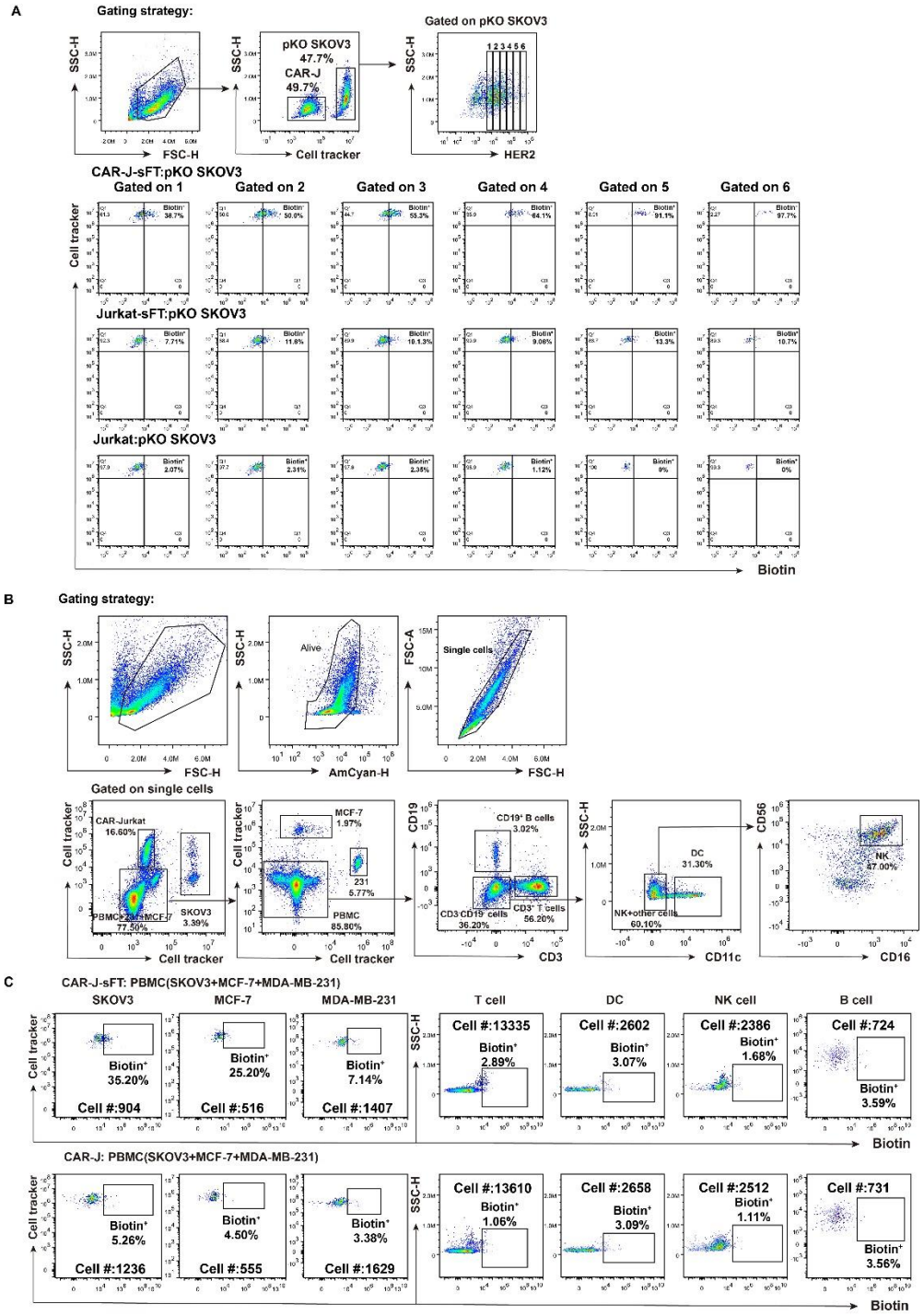

Fig. S7 Detection selectivity and quantity of interactions between Jurkat/CAR-J and SKOV3 via Jurkat/CAR-J-sFT. (A) Gating strategy and representative flow cytometric plots showing the biotinylated population of pKO SKOV3 with different HER2 expressions, in which CAR-J-sFT and Jurkat-sFT were using as bait cells respectively. The background is defined as the signal produced on Jurkat incubated with pKO SKOV3 without membrane-anchored sFT. The six group was divided manually according to the expression level of HER2. (B)(C) Gating strategy and representative flow cytometric plots showing biotinylation of SKOV3, MCF-7, MDA-MB-231, T cell, B cell, NK cell and DC in cell mixtures. (The ratio of SKOV3, MCF-7, MDA-MB-231 and PBMC is 1:1:1:10) The background is defined as the signal produced on SKOV3, MCF-7, MDA-MB-231, T cell, B cell, NK cell and DC by CAR-J without membrane-anchored sFT.

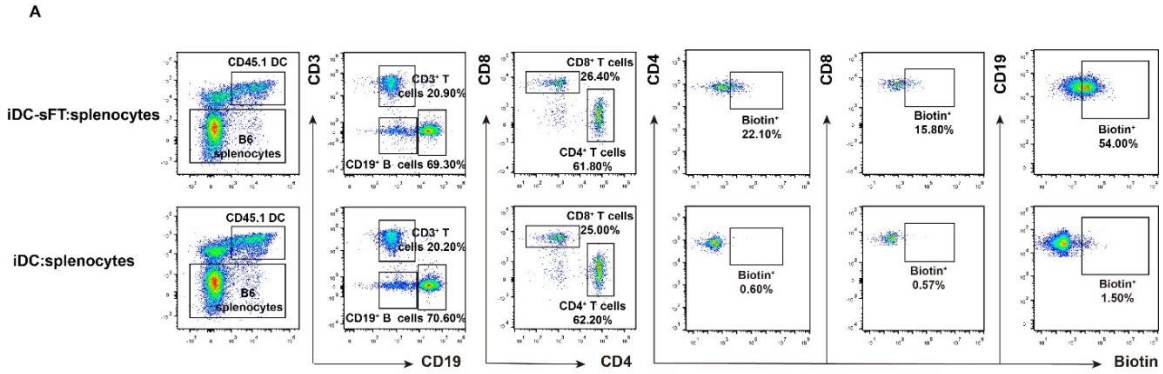

Fig. S8 Gating strategy for studying the interactions of iDC and splenocytes. (A) Gating strategy and representative flow cytometric plots showing biotinylation of immune cells in splenocytes. The background is defined as the signal produced on $CD4^+$ T cells, $CD8^+$ T cells and B cells by iDC without membrane-anchored sFT.

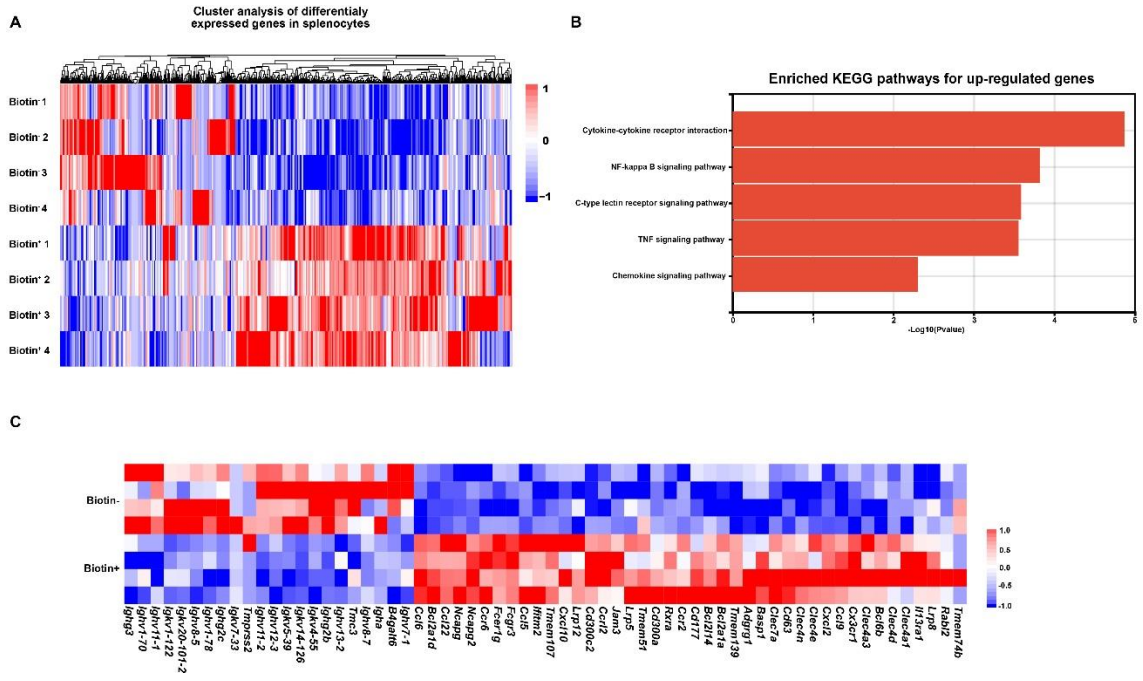

Fig. S9 Bioinformatic analysis of the distinct gene signatures of B cells interacting with iDC. (A) Cluster analysis of significantly differentially expressed genes between $Biotin^+$ and $Biotin^-$ B cells in splenocytes. (B) KEGG pathway enriched by the upregulated genes. Bar represents the P-value, n = 4. (C) Heatmap of differentially expressed genes between $Biotin^+$ and $Biotin^-$ B cells in splenocytes, n = 4. Focused on the gene set of membrane proteins.

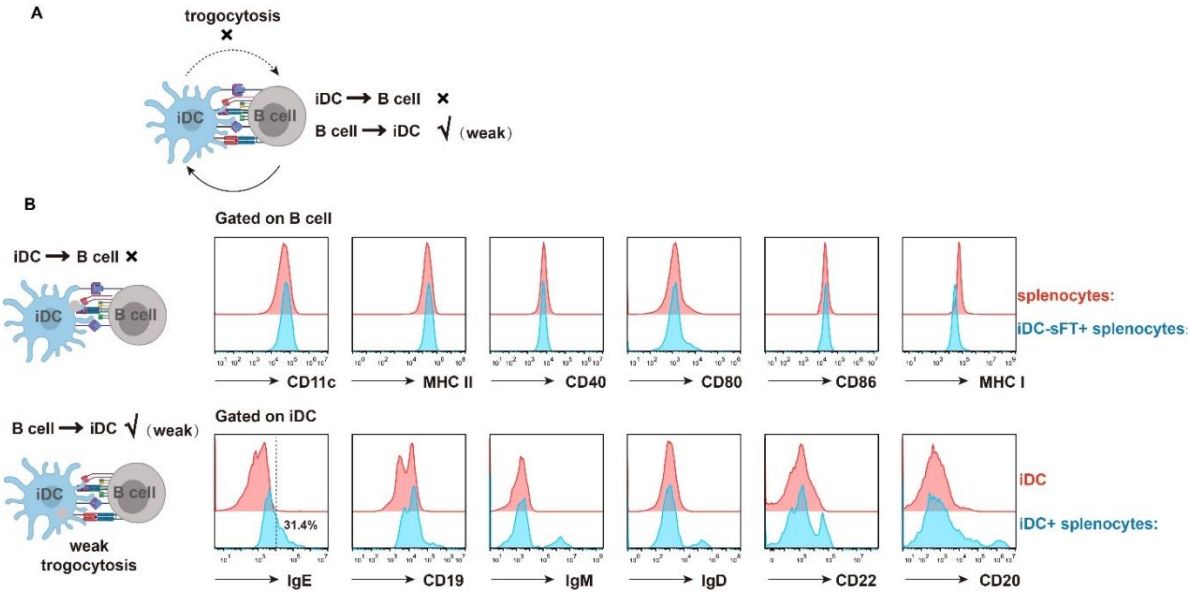

Fig. S10 Analysis of the interactions between iDCs and B cells via trogocytosis. (A) Schematic illustration of the interaction between iDCs and B cells revealed by the signal of trogocytosis. (B) Flow cytometric histograms showing of signal of trogocytosis appeared on cell surfaces. CD11c, MHC II, CD40, CD80, CD86 and MHC I are cell surface markers of DC, while IgE, IgM, IgD, CD19, CD22 and CD20 are cell surface markers of B cells.

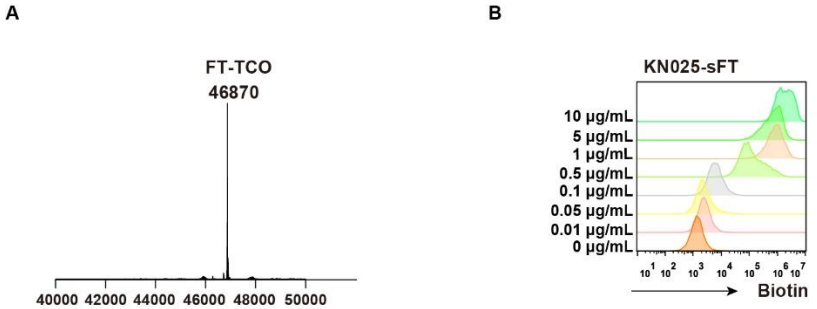

Fig. S11 Characterization of activity of KN025-sFT. (A) Characterization of site-specific FT-TCO by mass spectrum. (B) Characterization of activity of KN025-sFT by Fuc-Bio labeling on SKOV3.

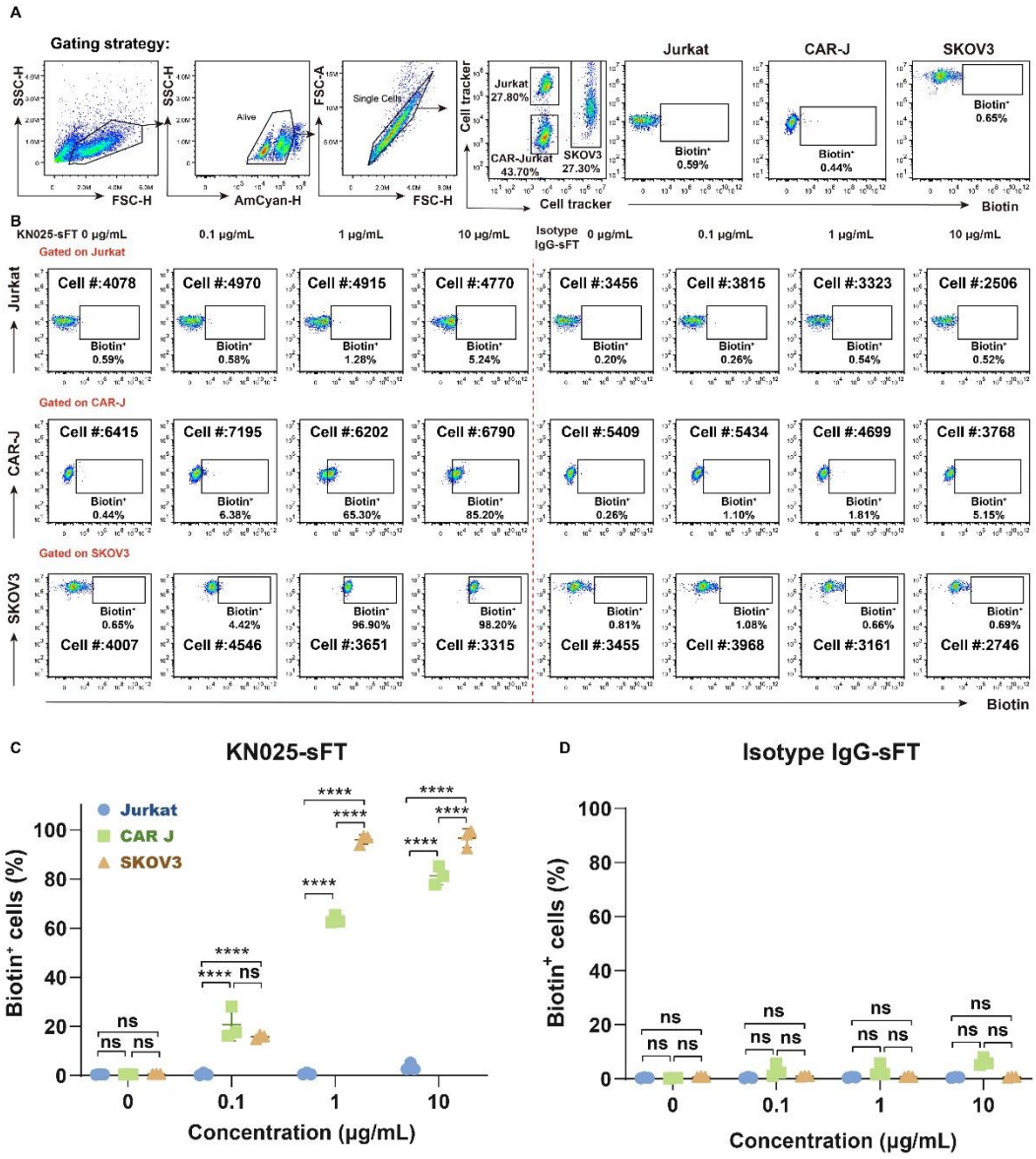

Fig. S12 Detection of interactions between Jurkat or CAR-J and SKOV3 via KN025-sFT. (A) Gating strategy and representative flow cytometric plots showing the background of Fuc-Bio labeling by without adding KN025-sFT. (B) Representative flow cytometric plots showing biotinylation of Jurkat, CAR-J and SKOV3 under different concentrations of KN025-sFT and Isotype IgG-sFT. (C) (D) Summary statistics of the interaction dependent Fuc-Bio of SKOV3, Jurkat and CAR-J in cell mixtures via KN025-sFT and Isotype IgG-sFT, n = 3. (ns $p > 0.05$; *$p < 0.05$; **$p < 0.05$; ****$p < 0.001$; ****$p < 0.0001$.)

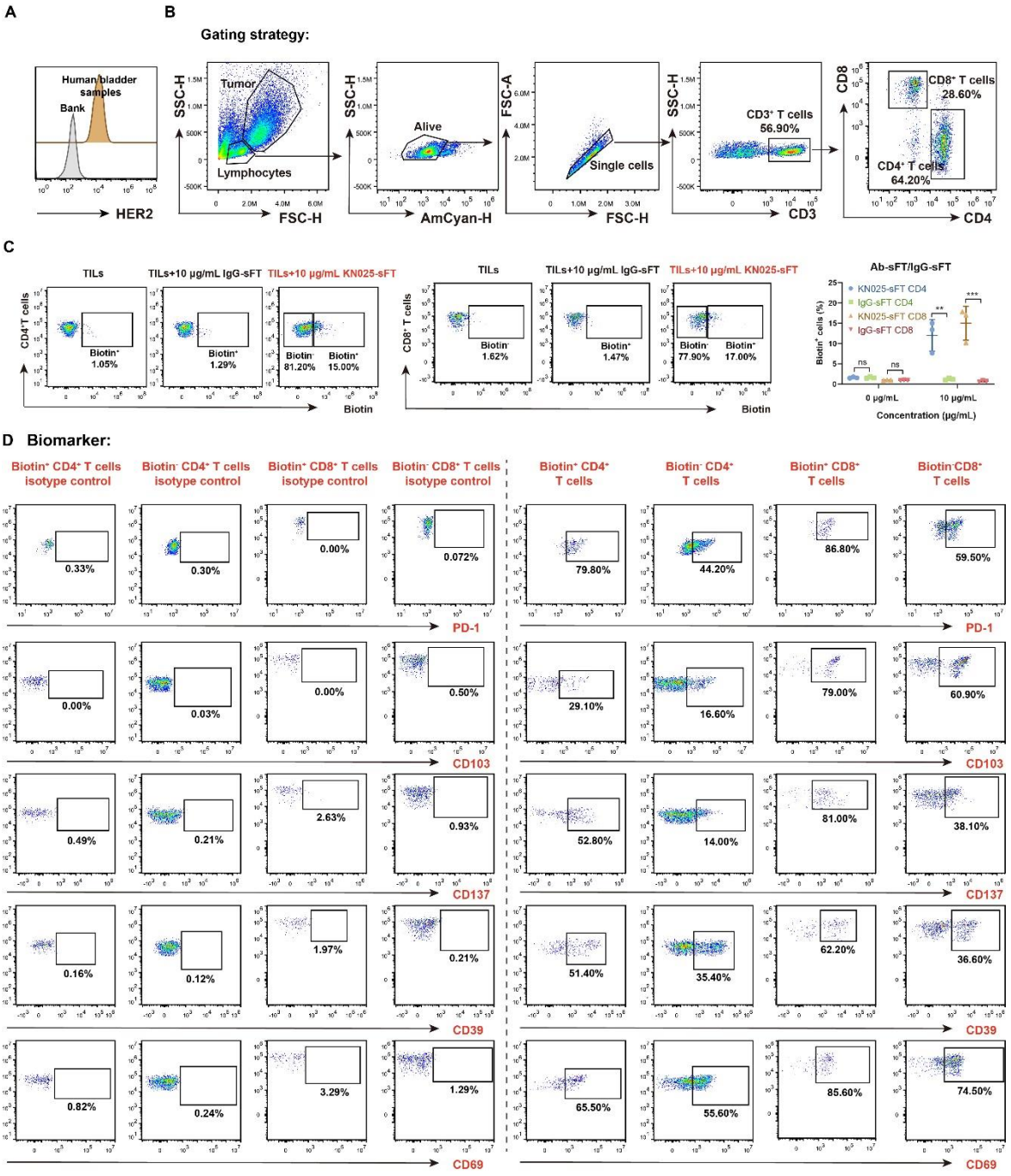

Fig. S13 Detection of interactions between cancer cells (HER2$^+$) and T cells in human bladder samples. (A) Flow cytometric characterization of HER2 expression level on human bladder cancer cells. (B) Representative flow cytometric plots showing the gating strategy for Fuc-Bio proportion of CD4$^+$ T cells and CD8$^+$ T cells in human bladder samples via KN025-sFT. (C) Flow cytometric analysis and summary statistics of the interaction dependent Fuc-Bio of CD4$^+$ T cells and CD8$^+$ T cells in human bladder samples via KN025-sFT and isotype IgG-sFT, n = 3. The background signal is defined as the signal produced on CD4$^+$ T cells and CD8$^+$ T cells by without adding KN025-sFT. (D) Flow cytometric plots showing the expression ratio of PD-1, CD103, CD137, CD39 and CD69 on Biotin$^+$ CD4$^+$ T cells, Biotin$^-$ CD4$^+$ T cells, Biotin$^+$ CD8$^+$ T cells and Biotin$^-$ CD8$^+$ T cells. The background signal is defined by Biotin$^+$ CD4$^+$ T cells, Biotin$^-$ CD4$^+$ T cells, Biotin$^+$ CD8$^+$ T cells and Biotin$^-$ CD8$^+$ T cells unstained for biomarkers. (ns $p > 0.05$; *$p < 0.05$; **$p < 0.05$; ****$p < 0.001$; ****$p < 0.0001$.)

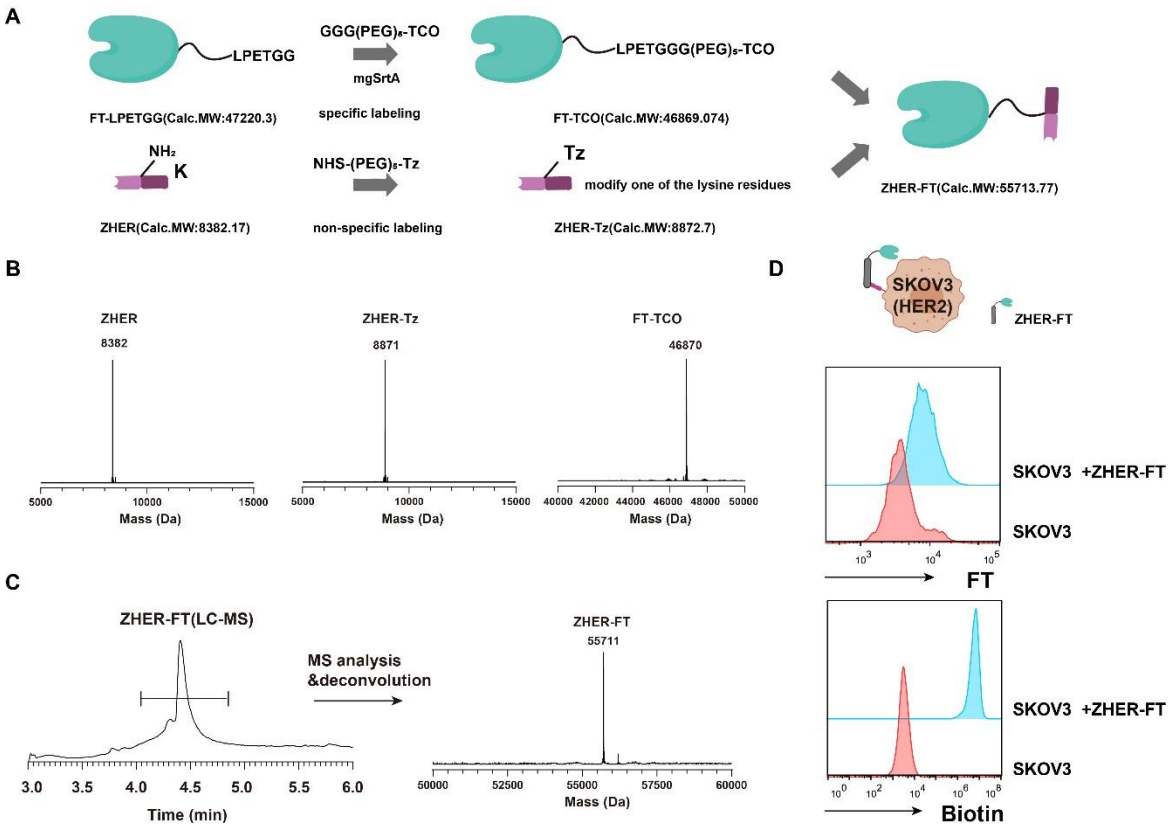

Fig. S14 Characterization of Nanobody-FT. (A) Schematic illustration of ZHER-FT construction. Calculated MWs of different parts are shown. (B) Characterization of ZHER, ZHER-Tz and FT-TCO by mass spectrum analysis. (C) Characterization of the ZHER-FT conjugate by LC-MS. Shown are detected MWs in B and C. (D) Characterization of the binding ability of ZHER-FT by anti-FT antibody and the activity of ZHER-FT on SKOV3 cells that triggers biotinylation on cell surface via GF-Biotin. Briefly, ZHER-FT was synthesized via the IEDDA mediated chemical ligation (see Supplementary Methods). SKOV3 cells were treated with ZHER-FT, which the binding of ZHER-FT on SKOV3 cells was confirmed by the anti-FT antibody. After that, SKOV3- ZHER-FT was incubated with 50 μM GF-Biotin to initiate the proximity labeling, which was confirmed by flow cytometry analysis after APC-SA (Streptavidin) staining.

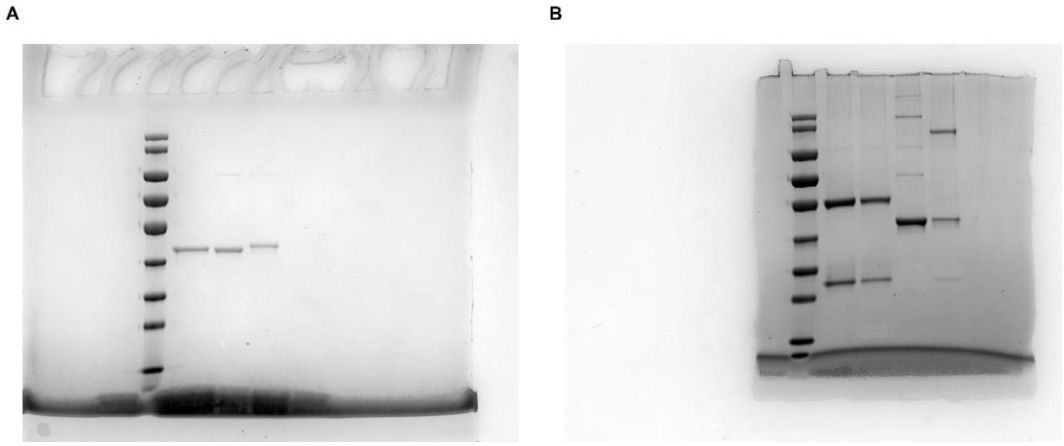

Fig. S15 High resolution non-cropped images of Coomassie gel.

Table S1.

Plasmid name	Protein sequence
FT-LPETGG on pET-28a (+)	MFQPLLDAFIESASIEKMVSKSPPPPLKIAVANWWGDEEIKEFKKSVLYFILS QRYAITLHQNPNESSDLVFSNPLGAARKILSYQNTKRVFYTGENESPNFNLF DYAIGFDELDFNDRYLRMPLYYAHLHYEAELVNDTTAPYKLKDNSLYALK KPSHHFKENHPNLSAVVNDESDLLKRGFASFVASNANAPMRNAFYDALNSI EPVTGGGSVRNTLGYKVGNKSEFLSQYKFNLCFENSQGYGYVTEKILDAYF SHTIPIYWGSPSVAKDFNPKSFVNVHDFNNFDEAIDYIKYLHTHPNAYLDML YENPLNTLDGKAYFYQDLSFKKILDFFKTILENDTIYHNNPFIFYRDLHEPLIS IDDLRVNYDDLRVNYDDLRVNYDDLRVNYLE**LPETGG**HHHHHH*
Herceptin 4D5 on pLenti	**MALPVTALLLPLALLLHAARP (CD8leader) YPYDVPDYA (HAtag)** GS**DIQMTQSPSSLSASVGDRVTITCRASQDVNTAVAWYQQKPGKAPKLL IYSASFLYSGVPSRFSGSRSGTDFTLTISSLQPEDFATYYCQQHYTTPPTF GQGTKVEIKRT (VL)** GGGGSGGGGSGGGGSGGGGS**EVQLVESGGGLVQPGGSLRLSCAASGFNI KDTYIHWVRQAPGKGLEWVARIYPTNGYTRYADSVKGRFTISADTSKN TAYLQMNSLRAEDTAVYYCSRWGGDGFYAMDYWGQGTLVTVSS (VH)** **GSEQKLISEEDL (Myc)** **FVPVFLPAKPTTTPAPRPPTPAPTIASQPLSLRPEACRPAAGGAVHTRGL DFACDIYIWAPLAGTCGVLLLSLVITLYCNHRN (human CD8 alpha chain 1 extracellular domain)** **KRGRKKLLYIFKQPFMRPVQTTQEEDGCSCRFPEEEEGGCEL (4-1BB)** **RVKFSRSADAPAYKQGQNQLYNELNLGRREEYDVLDKRRGRDPEMGG KPRRKNPQEGLYNELQKDKMAEAYSEIGMKGERRRGKGHDGLYQGLS TATKDTYDALHMQALPPR (CD3zeta)***
Human PD-1 on pLenti	MQIPQAPWPVVWAVLQLGWRPGWFLDSPDRPWNPPTFSPALLVVTEGDNA TFTCSFSNTSESFVLNWYRMSPSNQTDKLAAFPEDRSQPGQDCRFRVTQLPN GRDFHMSVVRARRNDSGTYLCGAISLAPKAQIKESLRAELRVTERRAEVPT AHPSPSPRPAGQFQTLVVGVVGGLLGSLVLLVWVLAVICSRAARGTIGARR TGQPLKEDPSAVPVFSVDYGELDFQWREKTPEPPVPCVPEQTEYATIVFPSG MGTSSPARRGSADGPRSAQPLRPEDGHCSWPL

Supplementary Methods

Synthesis procedure of ZHER-FT conjugates (ZHER-FT).

The Tz group was first introduced onto ZHER protein, which allows the production of ZHER-FT conjugates by a click reaction with FT-TCO. Briefly, a 50 mM stock of NHS-$(PEG)_4$-Tz in DMSO was added to solution of ZHER (7.4 mg/mL, 200 μL) at a final concentration of 5 mM. The solution was desalted into PBS by G25 desalting column to obtain 4 mg/mL ZHER-Tz. After that, 2 mg/mL FT-TCO was added to solution, (approximately 5 equiv. of ZHER-Tz) and incubated at room temperature for 5 min to obtain ZHER-FT.

Detection of the binding ability and activity of ZHER-FT.

A total of 1 million SKOV3 were resuspended in 100 μL HBSS buffer containing 20 mM $MgSO_4$, 3 mM HEPES and 0.5% FBS. Cells were treated with 0.2 mg/mL ZHER-FT, after incubated on ice for 30 min, SKOV3-sFT was washed twice with PBS. SKOV3-sFT cells were divided into two parts, one part was incubated with 10 μg/mL polyclonal FT antibody for 30 minutes on ice. After washing three times with PBS, PE anti-mouse IgG was used for flow cytometry to detect binding ability of ZHER-FT. The other part was added to 50 μM GF-Biotin and reacted on ice for 20 minutes. After washing twice with PBS, APC-SA (Streptavidin) was used for flow cytometry to detect labeling activity of FT.

Luminescent cell viability assay

10000 MC38 or MB49 cancer cells (stable luciferase expression) presented $OVA_{257-264}$ were seeded into 96-well plates, and 200000 OT-I $CD8^+$T cells were added and incubated for 24 hours. CellTiter-Glo Reagent (Promega) was added after 24 h incubation. Luminescent signal was determined using Synergy 2 MultiMode Microplate Reader.

Spectra

1. *Synthesis of GDP-Fuc-AM -Biotin*

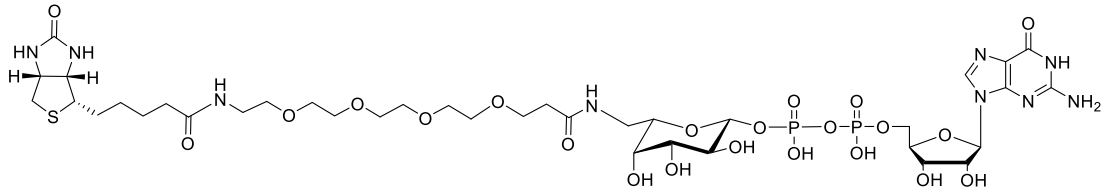

500 μL GDP-Fuc-AM (100 mM in ddH_2O) in 1.5 mL ddH_2O were added with 500 μL $NaHCO_3$ (200 mM), 1.95 mL THF and 550 μL NHS-PEG_4-Biotin (Click Chemistry Tools) (100 mM in THF). The reaction was stirred at r.t. for 4 h and monitored by TLC. The solvent was removed under reduced pressure. The crude product was further purified through a Prep-HPLC system to give the product as a white solid (20.5 mg, 38%). HRMS (ESI-) calcd for $C_{37}H_{61}N_9O_{22}P_2S$ ($M-H^+$) 1076.3054, found 1076.3068. **^{1}H NMR** (400 MHz, D_2O) δ 8.13 (s, 1H), 5.93 (d, *J* = 6.1 Hz, 1H), 4.94 (t, *J* = 7.8 Hz, 1H), 4.80-4.78 (m, 1H), 4.59 (dd, *J* = 7.9, 4.6 Hz, 1H), 4.54 (dd, *J* = 5.2, 3.4 Hz, 1H), 4.40 (dd, *J* = 7.9, 4.4 Hz, 1H), 4.36-4.35 (m, 1H), 4.23 (dd, *J* = 5.4, 3.4 Hz, 2H), 3.88 (d, *J* = 3.1 Hz, 1H), 3.77 (t, *J* = 6.3 Hz, 2H), 3.69-3.67 (m, 14H), 3.64-3.62 (m, 3H), 3.6-3.58 (m, 1H), 3.39 (t, *J* = 5.3 Hz, 2H), 3.33-3.27 (m, 2H), 2.98 (dd, *J* = 13.1, 5.0 Hz, 1H), 2.78 (d, *J* = 13.0 Hz, 1H), 2.57 (t, *J* = 6.2 Hz, 2H), 2.27 (t, *J* = 7.3 Hz, 2H), 1.76-1.54 (m, 4H), 1.43-1.37 (m, 2H). **^{13}C NMR** ^{13}C (101 MHz, D_2O) δ 176.9, 174.2, 165.3, 158.8, 153.9, 151.8, 116.2, 98.5, 98.4, 86.8, 83.8, 83.7, 73.64, 73.55, 72.14, 71.16, 71.07, 70.44, 69.61, 69.58, 69.56, 69.53, 69.39, 68.98, 68.86, 66.75, 65.33, 65.28, 62.04, 60.23, 55.33, 40.0, 38.89, 35.70, 35.44, 27.87, 27.67, 25.12.

Mass spectrometry

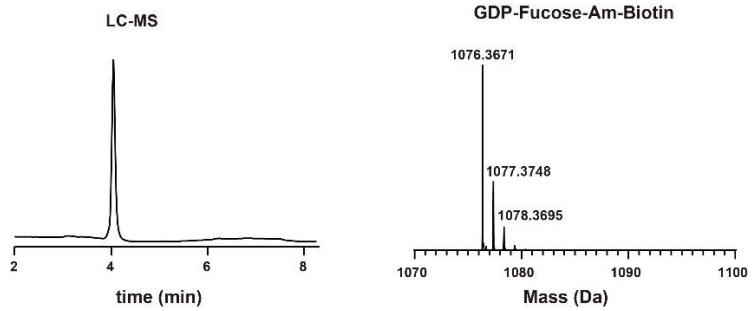

^{1}H NMR (400 MHz, D_2O)

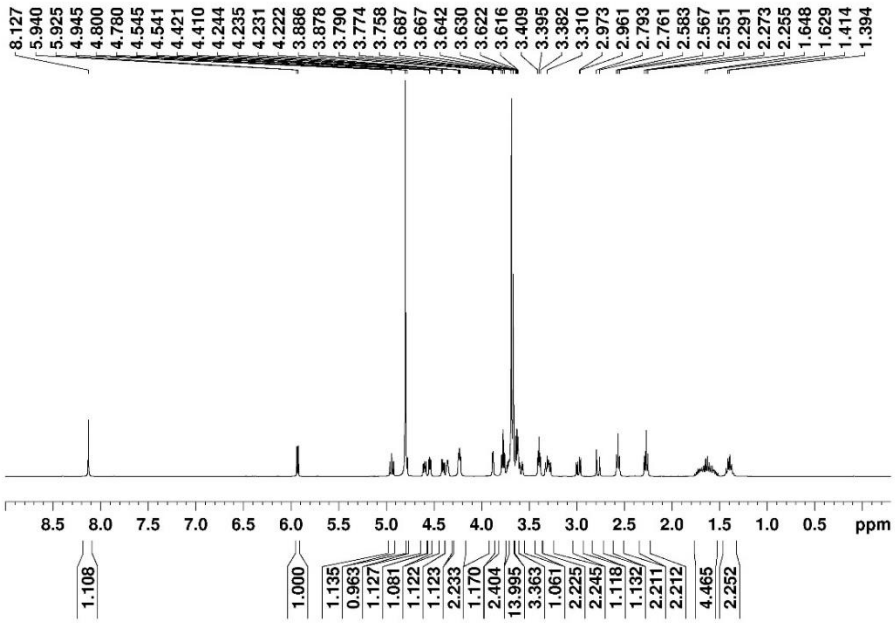

^{13}C NMR (101 MHz, D_2O)

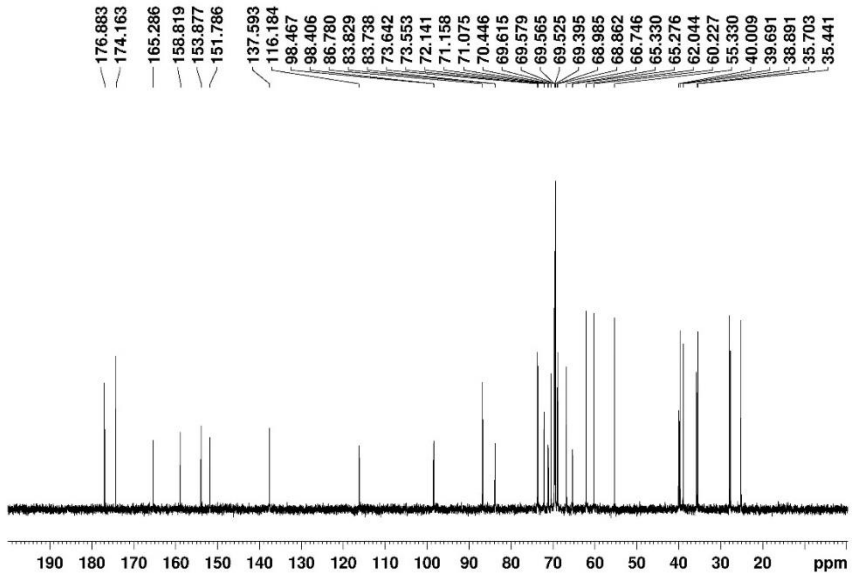

2. Synthesis of GDP-Fuc-AM- BCN

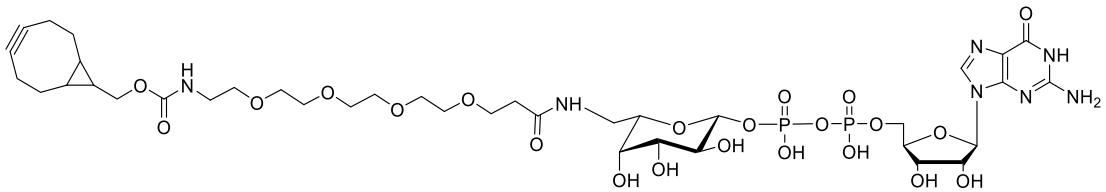

200 μL GDP-Fuc-AM (100 mM) in 600 μL ddH_2O were added with 200 μL $NaHCO_3$ (200 mM), 560 μL THF and 440 μL NHS-PEG_4-BCN (Xi'an Dianhua Biotechnology Co.,Ltd) (50 mM in THF). The reaction was stirred at rt for 4 h and monitored by TLC. The solvent was removed under reduced pressure. The crude product was further purified through a Prep-HPLC system to give the product as a white solid (7.4 mg, yield 36%). HRMS (ESI-) calcd for $C_{38}H_{59}N_7O_{22}P_2$ (M-2H$^+$)/2 512.6522, found 512.6532. **^{1}H NMR** (400 MHz, D_2O) δ 8.17 (s, 1H), 5.92 (d, *J* = 5.9 Hz, 1H), 4.93 (t, *J* = 7.8 Hz, 1H), 4.78-4.75 (m, 1H), 4.52 (dd, *J* = 5.1, 3.5 Hz, 1H), 4.36-4.32 (m, 1H), 4.22 (dd, *J* = 5.4, 3.4 Hz, 2H), 4.14 (d, *J* = 8.2 Hz, 2H), 3.86 (d, *J* = 2.3 Hz, 1H), 3.75 (t, *J* = 6.3 Hz, 2H), 3.69-3.64 (m, 14H), 3.62-3.58 (m, 4H), 3.31 (t, *J* = 5.3 Hz, 2H), 3.29-3.26 (m, 1H), 2.55 (t, *J* = 6.2 Hz, 2H), 2.29-2.15 (m, 6H), 1.54-1.51 (m, 2H), 1.39-1.31 (m, 1H), 0.92 (t, *J* = 9.8 Hz, 2H). **^{13}C NMR** (100 MHz, CDCl3): 174.15, 158.76, 158.56, 153.97, 151.61, 137.43, 115.69, 100.18, 98.47, 98.40, 87.0, 83.79,83.70, 78.73, 73.56, 72.14, 71.16, 71.08, 70.35,69.58, 69.52, 69.42, 69.40, 69.33, 68.98, 66.74, 65.25, 65.19, 63.72, 40.0, 35.70, 20.70, 19.69, 17.14

Mass spectrometry

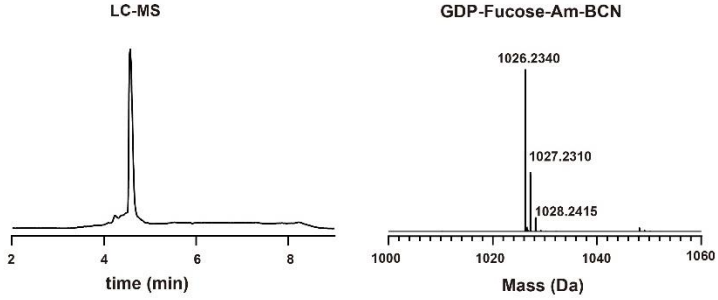

^{1}H NMR (400 MHz, D2O)

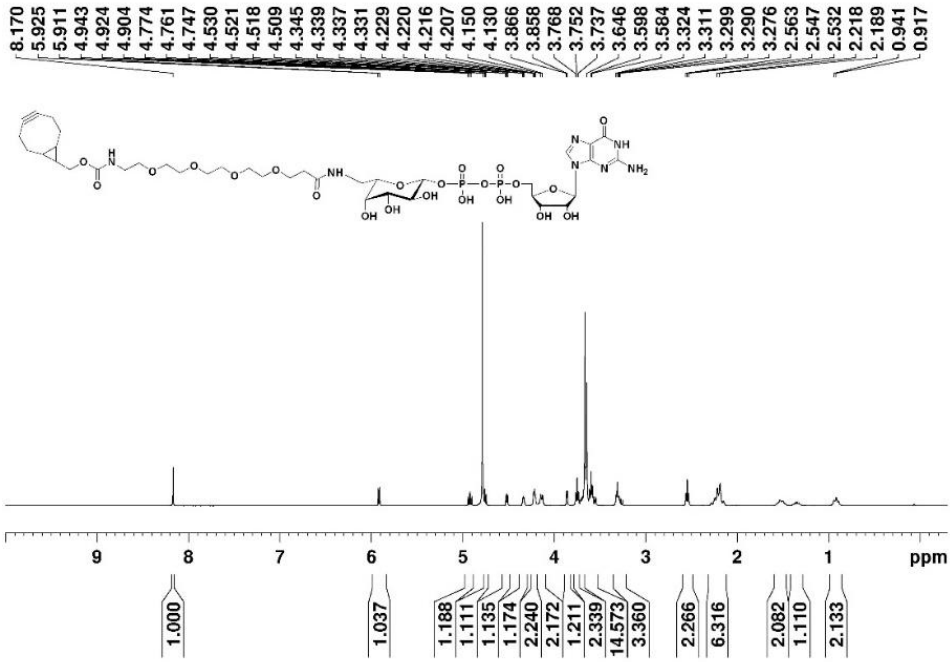

^{13}C NMR (100 MHz, CDCl3)